

Fluctuation-dissipation relations outside the linear response regime in a two-dimensional driven lattice gas along the direction transverse to the driving force

Kumiko Hayashi

Department of Pure and Applied Sciences, University of Tokyo, Komaba, Tokyo 153-8902, Japan

(Dated: February 8, 2020)

We performed numerical experiments on a two-dimensional driven lattice gas, which constitutes a simple stochastic nonequilibrium many-body model. In this model, focusing on the behavior along the direction transverse to the external driving force, we numerically measure transport coefficients and dynamical fluctuations outside the linear response regime far from equilibrium. Using these quantities, we find the validity of the Einstein relation, the Green-Kubo relation and the fluctuation-response relation.

PACS numbers: 05.70.Ln, 05.40.-a

In order to construct a theoretical framework of nonequilibrium statistical mechanics, we seek new universal relations characterizing nonequilibrium steady states (NESS) far from equilibrium. For this purpose, we carry out numerical computations through which we study the validity of certain fluctuation-dissipation relations. In this paper, we consider one such model, a simple stochastic nonequilibrium many-body model which is called a 'driven lattice gas (DLG)' [1, 2].

Model: Let η_i be an occupation variable defined on each site $i = (i_x, i_y)$ of a two-dimensional square lattice $\{(i_x, i_y) | 0 \leq i_x \leq L, 0 \leq i_y \leq L\}$. The variable η_i is 1 if the i -th site is occupied by a particle, and 0 if it is unoccupied. Periodic boundary conditions are imposed by setting $\eta_i = \eta_j$, where $j = (L, i_y)$ in the case $i_x = 0$, and $\eta_i = \eta_j$, where $j = (i_x, L)$ in the case $i_y = 0$. The array of all occupation variables, $\{\eta_i\}$, is denoted $\boldsymbol{\eta}$ and called the "configuration".

The time evolution of $\boldsymbol{\eta}$ is described by the following rule: At each time step, randomly choose a nearest-neighbor pair $\langle i, j \rangle$, and exchange the values of η_i and η_j with the probability $c(i, j; \boldsymbol{\eta}) = (1 + \exp[\beta Q(\boldsymbol{\eta} \rightarrow \boldsymbol{\eta}^{ij})])^{-1}$, where $\boldsymbol{\eta}^{ij}$ is the configuration obtained from $\boldsymbol{\eta}$ through this exchange, and $\beta = 1/T$ is the inverse temperature with the Boltzmann constant set to unity. $Q(\boldsymbol{\eta} \rightarrow \boldsymbol{\eta}^{ij})$ represents the heat absorbed from the heat bath as a result of the configuration change $\boldsymbol{\eta} \rightarrow \boldsymbol{\eta}^{ij}$. The total particle number, $N = \sum_i \eta_i$, is conserved throughout the time evolution. The density $\rho = N/L^2$ is a parameter of the model. Hereafter, we regard the unit of time to be L^2 time steps, which is the number of time steps for which an arbitrary site is chosen once on average. We refer to this time as 1 MCS (Monte Carlo step per site).

In this paper, we study a two-dimensional DLG with

$$Q(\boldsymbol{\eta} \rightarrow \boldsymbol{\eta}') \equiv H_0(\boldsymbol{\eta}') - H_0(\boldsymbol{\eta}) - E j_p(\boldsymbol{\eta} \rightarrow \boldsymbol{\eta}'), \quad (1)$$

where E is an external driving force, and $H_0(\boldsymbol{\eta})$ describes an interaction between particles, written $H_0(\boldsymbol{\eta}) \equiv -\sum_{\langle i, j \rangle} \eta_i \eta_j$, where $\langle i, j \rangle$ denotes a nearest-neighbor pair. The quantity $j_p(\boldsymbol{\eta} \rightarrow \boldsymbol{\eta}')$ is the spatially-averaged current, that is, the net number of particles flowing in

the x -direction: $j_p(\boldsymbol{\eta} \rightarrow \boldsymbol{\eta}') \equiv \sum_i [\eta_i (1 - \eta'_i) \eta'_{i+(1,0)} (1 - \eta_{i+(1,0)}) - \eta'_i (1 - \eta_i) \eta_{i+(1,0)} (1 - \eta'_{i+(1,0)})]$. In this study, we fix $\beta = 0.5$ in order for the system to be far from the critical region (Note that the critical temperature of the model with $E = 0$ is $\beta_c = 1.76$.), and choose large values of E in order for the system to be far from equilibrium.

Our aim: In DLGs, regarded as one of the simplest classes of nonequilibrium models, statistical properties of NESS have been investigated from various points of view. Among them, there is an interesting report that a large deviation functional of density fluctuations is shape dependent [3]. In a two-dimensional DLG, although the general properties of fluctuations are quite different from those of equilibrium states, it was found numerically that a fluctuation relation holds [4], where we consider only properties along the direction transverse to the external force E . This fluctuation relation is a relation among density fluctuations, the chemical potential [5, 6], and the temperature of the environment.

In equilibrium cases, the fluctuation relation is closely related to fluctuation-dissipation relations, which relate dynamical properties of equilibrium fluctuations with transport properties in the linear response regime [7]. Then noting that the fluctuation relation holds in the DLG even far from equilibrium [4], we wish to also investigate the validity of fluctuation-dissipation relations far from equilibrium, and determine if their equilibrium forms hold here as well.

In order to obtain such relations, we directly measure transport coefficients and dynamical fluctuations in the direction transverse to the driving force E in the two-dimensional DLG investigated above. In spite of the fact that these measured values differ from those for the equilibrium state ($E = 0$), we numerically find that three fluctuation-dissipation relations, the Einstein relation, the fluctuation-response relation, and the Green-Kubo relation, seem to be valid even for NESS far from equilibrium.

Einstein relation: In the linear response regime near $E = 0$, the Einstein relation for interacting many-body systems is written

$$D\chi = \sigma T, \quad (2)$$

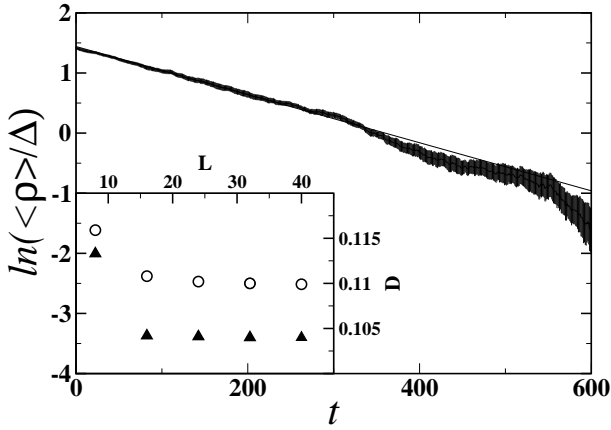


FIG. 1: The quantity $\ln(-\langle\hat{\rho}(t)\rangle_{E,\epsilon=0}^V/\Delta)$ plotted as a function of t in the case $(\rho, E) = (0.5, 10)$, with $\Delta = -0.2$, $L = 32$. From the slope of the line, $-0.004t + 1.44$, D is estimated as $0.004 = D(2\pi/L)^2$. The inset displays the L dependence of D . The triangle and circle correspond to $(\rho, E) = (0.5, 10)$ and $(0.5, 0)$, respectively.

where D is the density diffusion constant, χ is the intensity of density fluctuations, and σ is the conductivity [8].

In order to investigate the validity of (2) in the direction transverse to the external driving force E (the y -direction), we first need to define the density diffusion constant D as the coefficient of the diffusion term in the evolution equation describing the averaged behavior of a density field in this direction. In this paper, we consider the case in which we have prepared as the initial state, a steady state under the perturbation potential

$$V(i_y) = \Delta \sin \frac{2\pi i_y}{L} \quad (3)$$

which is obtained by adding $\sum_i \eta_i V(i_y)$ to $H_0(\boldsymbol{\eta})$. Then, we remove $V(i_y)$ at $t = 0$ in order to measure the relaxation of the density field $\hat{\rho}(t)$. The function $\hat{\rho}(t)$ is the Fourier transform of the coarse-grained density $\rho(i_y)$. These quantities are defined as $\hat{\rho}(t) \equiv \sum_{i_y=1}^L \rho(i_y) \sin \frac{2\pi i_y}{L}$, and $\rho(i_y) \equiv \frac{1}{L} \sum_{i \in \Omega_{i_y}} \eta_i$, where $\Omega_{i_y} = [1 \leq i_x \leq L, i_y]$.

In Fig. 1, choosing Δ as a sufficiently small value, $\ln(-\langle\hat{\rho}(t)\rangle_E^V/\Delta)$ is plotted as a function of t in the case $(\rho, E) = (0.5, 10)$ with $L = 32$ and $\Delta = -0.2$. Here, $\langle \rangle_E^V$ represents the statistical average under the relaxation process. Because exponentially decaying behavior of $\langle\hat{\rho}(t)\rangle_E^V$ is observed, D can be estimated from the form

$$\langle\hat{\rho}(t)\rangle_E^V = \text{const.} \cdot e^{-D(\frac{2\pi}{L})^2 t}. \quad (4)$$

In the inset of Fig. 1, D is plotted as a function of the system size L in the cases $E = 0$ and $E = 10$, with $\rho = 0.5$. Because both values of D seem to converge, we conclude

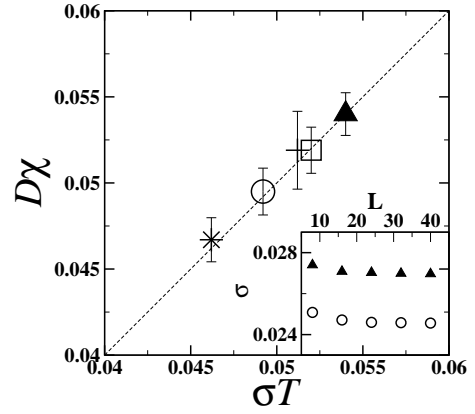


FIG. 2: σT as a function of $D\chi$. The triangle, square, star, plus, and circle correspond to $(\rho, E) = (0.5, 10), (0.4, 10), (0.3, 10), (0.5, 3)$ and $(0.5, 0)$. The error bars represent the statistical errors arising from the fitting when D is measured. The thin-dotted line represents $D\chi = \sigma T$. The inset displays the L dependence of σ . The triangles and circles correspond to $(\rho, E) = (0.5, 10)$ and $(0.5, 0)$, respectively.

that the size $L = 40$ can be regarded as sufficiently large to study the statistical properties of macroscopic quantities in our model. It is important to note here that the values of D in the case $E = 10$ are different from those in the case $E = 0$.

Next, we define the conductivity $\bar{\sigma}$ by adding a sufficiently small perturbative driving force ϵ in the y -direction. This is realized by adding the term $\epsilon j_t(\boldsymbol{\eta} \rightarrow \boldsymbol{\eta}')$ to $Q(\boldsymbol{\eta} \rightarrow \boldsymbol{\eta}')$ in (1), where

$$j_t(\boldsymbol{\eta} \rightarrow \boldsymbol{\eta}') \equiv \sum_i [\eta_i(1 - \eta'_i)\eta'_{i+(0,1)}(1 - \eta_{i+(0,1)}) - \eta'_i(1 - \eta_i)\eta_{i+(0,1)}(1 - \eta'_{i+(0,1)})]. \quad (5)$$

Note that in the x -direction, the particles are still driven by E . Then, the averaged current \bar{J}_ϵ in the y -direction is defined as

$$\bar{J}_\epsilon \equiv \frac{1}{L} \langle j_t(\boldsymbol{\eta} \rightarrow \boldsymbol{\eta}') \rangle_s^{E,\epsilon}. \quad (6)$$

Using this \bar{J}_ϵ , the conductivity σ is written

$$\sigma \equiv \lim_{\epsilon \rightarrow 0} \frac{\bar{J}_\epsilon}{\epsilon}. \quad (7)$$

In the inset of Fig. 2, σ is plotted as a function of the system size, L , in the cases $E = 0$ and $E = 10$ with $\rho = 0.5$. Note that the values of σ in the case $E = 0$ are smaller than those in the case $E = 10$, and that qualitatively, this difference is not the same as that seen for D .

We previously measured the intensity of density fluctuations $\chi \equiv L\ell(\langle\rho_\ell^2\rangle_s^E - (\langle\rho_\ell\rangle_s^E)^2)$, where $\rho_\ell \equiv \sum_{i \in \Omega_\ell} \eta_i/|\Omega_\ell|$ and $\Omega_\ell = \{(i_x, i_y) | 1 \leq i_x \leq L, L/2 - \ell/2 -$

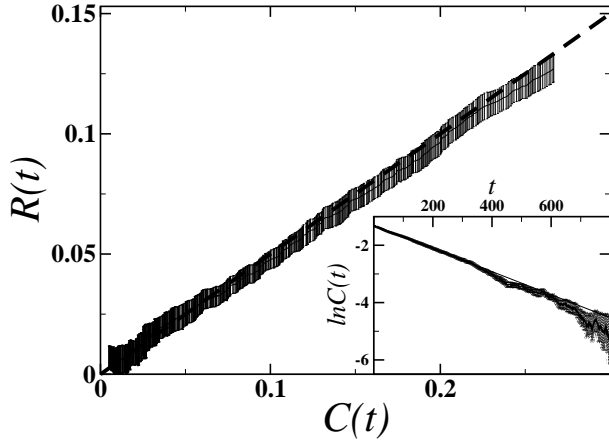


FIG. 3: $R(t)$ plotted as a function of $C(t)$ in the case $(\rho, E) = (0.5, 10)$, with $L = 32$ and $\Delta = -0.2$ over the interval $0 \leq t \leq 800$ MCS. The line represents $R(t) = \beta C(t)$, where $T = 2(\beta = 0.5)$. The error bars represent these of $R(t)$, because the uncertainty on $C(t)$ is smaller. In the inset, $\ln C(t)$ is plotted. The line there represents $-0.00403t - 1.31$.

$1 \leq i_y \leq L/2 + \ell/2$ }. (See Fig. 4 in Ref. [4].) Note that ℓ is chosen so that it satisfies $\xi \ll \ell \ll L$ where ξ is a correlation length. Using these values of χ , in Fig. 2, we plot σT as a function of $D\chi$ in the cases $(\rho, E) = (0.5, 10), (0.4, 10), (0.3, 10), (0.5, 3)$ and $(0.5, 0)$. Noting that the thin-dotted line represents $D\chi = \sigma T$, we find that even though the values of D , σ and χ are different from those in the equilibrium case, along the direction transverse to the driving force E , the Einstein relation (2) is valid, within the precision of the numerical computations.

Fluctuation-response relation: We next study in the fluctuation-response relation, which is also a representative universal relation in the linear response theory. Again in this case, we focus on the properties of the system in the direction transverse to the driving force E .

First, we employ the same procedure as in the measurement of D to introduce a time dependent response function $R(t)$. That is, we prepare the steady state under the perturbation $V(i_y)$ and then remove this perturbation at $t = 0$. Because the profile of the coarse grained density $\rho(i_y)$ is changed by the removal of $V(i_y)$, we make this change explicit by defining $R(t)$ in the following form:

$$R(t) \equiv -\frac{\langle \hat{\rho}(t) \rangle_E^V}{L\Delta}. \quad (8)$$

We remark that the decaying behavior of $R(t)$ in the case $E = 10$ is plotted as that of $-\langle \hat{\rho}(t) \rangle_E^V / \Delta$ in Fig. 1.

Next, we introduce the time correlation function of density fluctuations in the direction transverse to the driving force:

$$C(t) \equiv \langle \hat{\rho}(t) \hat{\rho}(0) \rangle_s^E. \quad (9)$$

In the inset of Fig. 3, $\ln C(t)$ is plotted as a function of

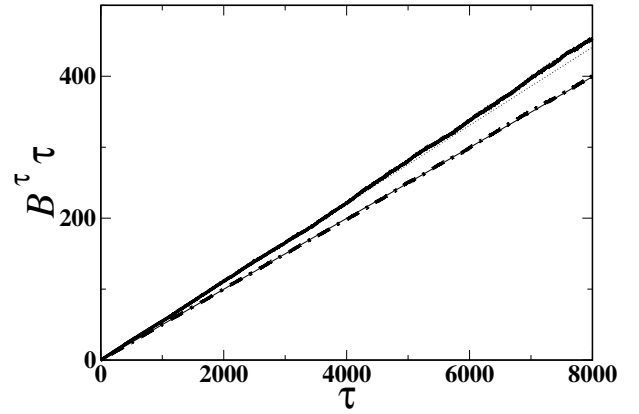


FIG. 4: $B^\tau \tau$ plotted as a function of τ in the case $(\rho, E) = (0.5, 0)$ (the dotted line) and $(\rho, E) = (0.5, 10)$ (the straight line) with $L = 32$. The thin line represents 0.050τ and the thin dotted line represents 0.055τ . In the case $E = 10$, it is seen that the line deviates from the thin dotted line at large t MCS.

time in the case $E = 10$, with $\rho = 0.5$ and $L = 32$. For the NESS, $C(t)$, like $R(t)$ decays exponentially in time.

Here, in the equilibrium case ($E = 0$), using $R(t)$ and $C(t)$, the fluctuation-response relation is given by

$$C(t) = TR(t). \quad (10)$$

In the NESS far from equilibrium studied here, because $R(t)$ and $C(t)$ exhibit a similar behavior, and because the fluctuation relation, which is essentially the same as $C(0) = TR(0)$, has previously been found to hold [4], we conjecture that (10) is valid.

To demonstrate its validity explicitly, in Fig. 3, in the case $E = 10$ with $\rho = 0.5$ and $L = 32$, $R(t)$ is plotted as a function of $C(t)$ over the interval $0 \leq t \leq 800$ MCS. It is seen that the slope is equal to $1/T$, within the precision of the numerical computations.

Green-Kubo relation: Finally, again considering the properties along the direction transverse to the external driving force (the y -direction), we investigate the validity of the Green-Kubo relation for NESS far from equilibrium.

Using the spatially-averaged current in the direction transverse to the external driving force, j_t , defined in (5), we begin by the τ dependent current J^τ , which represents the net number of particles that move in the y -direction during a time of τ MCS,

$$J^\tau \equiv \frac{1}{\tau L^2} \sum_{k=1}^{\tau L^2} j_t(\boldsymbol{\eta}(k-1) \rightarrow \boldsymbol{\eta}(k)). \quad (11)$$

Then, using this expression for J^τ , the intensity of the current fluctuations is defined by

$$B^\tau \equiv \frac{\tau L^2}{2} \langle (J^\tau)^2 \rangle_s^E. \quad (12)$$

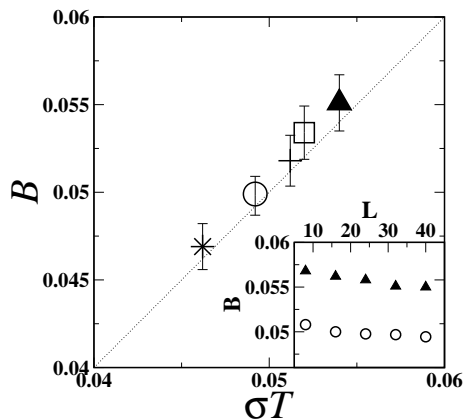


FIG. 5: σT as a function of B . The triangle, square, star, plus, and circle correspond to $(\rho, E) = (0.5, 10), (0.4, 10), (0.3, 10), (0.5, 3)$ and $(0.5, 0)$. The inset displays the L dependence of B . The triangles and circles correspond to $(\rho, E) = (0.5, 10)$ and $(0.5, 0)$, respectively.

In Fig 4, $B^T \tau$ is plotted as a function of τ in the cases $E = 0$ and $E = 10$, with $\rho = 0.5$ and $L = 32$, respectively. It is seen that in the case $E = 10$, the line fitted for small times (but much larger than the relaxation time of the current correlations) deviates slightly for large times, while in the case $E = 0$, $B^T \tau$ and 0.050τ are equal within the numerical precision for all times. This bending behavior of $B^T \tau$ might reflect the effect of a long time tail in this NESS.

In the case $E = 0$, defining B as the slope of $B^T \tau$, the Green-Kubo relation [8] can be written

$$B = \sigma T. \quad (13)$$

In the case $E \neq 0$, we define B as the slope of $B^T \tau$ obtained from the fitting in the early time regime. With this definition, the size dependence of B in the cases $E = 0$ and $E = 10$ with $\rho = 0.5$ is plotted in the inset of Fig. 5. The difference between the values of B in the cases $E = 0$ and $E = 10$ is qualitatively the same as that for

σ .

Considering this similarity between σ and B , in Fig. 5, we plot σT as a function of B in the cases $(\rho, E) = (0.5, 0), (0.5, 10), (0.5, 3), (0.4, 10), (0.3, 10)$ with $L = 32$. The Green-Kubo relation (13) is valid for the NESS considered here. However, the deviation seen in Fig. 5 is somewhat larger than that in Fig. 2.

Summary: In this paper, we have reported the results of numerical experiments on the two-dimensional DLG focusing on the properties along the direction transverse to the external driving force E . We find that the Einstein relation, the fluctuation-response relation and the Green-Kubo relation hold in the NESS far from equilibrium. (Note that the validity of the fluctuation relation for such a state was previously demonstrated in Ref. [4].)

Compared with this validity of relations in the direction transverse to the external driving force, we remark the properties along the direction parallel to the external driving force. We studied a one-dimensional DLG, and found that the phenomena observed along the direction parallel to the external driving force seemed to be more complicated than those observed along the direction transverse to the external driving force [9].

We end with some discussion of the detailed balance of fluctuations, which has a deep connection with the validity of universal relations in the linear response regime near equilibrium states. In our DLG, the detailed balance condition for $c(i, j; \boldsymbol{\eta})$ does not hold in the case $E \neq 0$. However, the numerical confirmation of the universal relations presented here suggests the detailed balance of macroscopic fluctuations. We point out that, with regard to this topic, D. Gabielli et al. studied a stochastic model for which the detailed balance condition does not hold, and derived the Onsager's reciprocity, which is also the linear response relations for macroscopic quantities [10].

The author acknowledges S. Sasa and H. Tasaki for discussions on NESS. This work was supported by a JSPS Research Fellowship for Young Scientists (Grant No. 1711222).

[*] Electronic address: hayashi@jiro.c.u-tokyo.ac.jp

[1] B. Schmittman and R. K. P Zia *Phase transitions and Critical Phenomena Volume 17, Statistical Mechanics of Driven Diffusive Systems* (Academic Press, 1995); J. Marro and R. Dickman *Nonequilibrium Phase Transitions in Lattice Models* (Cambridge University Press, 1999)
 [2] S. Katz, J. L. Lebowitz, H. Spohn, J. Stat. Phys. **34**, 497, (1984).
 [3] F. J. Alexander and G. L. Eyink, Phys. Rev. **E 57**, 6229 (1998).
 [4] K. Hayashi and S. Sasa, Phys. Rev. E **68**, 035104(R)

(2003).

[5] This chemical potential was defined operationally. The theoretical background employed in [4] is supported by the result of Ref. [6].
 [6] S. Sasa and H. Tasaki, e-print cond-mat/0411052.
 [7] K. Hayashi and S. Sasa, e-print cond-mat/0507719.
 [8] R. Kubo, Rep. Prog. Phys. **29** 255, (1966).
 [9] K. Hayashi and S. Sasa, Phys. Rev. E **71**, 046143 (2005).
 [10] D. Gabielli, G. Jona-Lasinio, C. Landim, Phys.Rev.Lett. **77**, 1202, (1996)